



Anisotropic superconducting spin transport at magnetic interfacesYuya Ominato ¹, Ai Yamakage,² and Mamoru Matsuo ^{1,3,4,5}¹*Kavli Institute for Theoretical Sciences, University of Chinese Academy of Sciences, Beijing 100190, China*²*Department of Physics, Nagoya University, Nagoya 464-8602, Japan*³*CAS Center for Excellence in Topological Quantum Computation, University of Chinese Academy of Sciences, Beijing 100190, China*⁴*Advanced Science Research Center, Japan Atomic Energy Agency, Tokai 319-1195, Japan*⁵*RIKEN Center for Emergent Matter Science (CEMS), Wako, Saitama 351-0198, Japan*

(Received 13 February 2022; accepted 29 September 2022; published 14 October 2022)

We present a theoretical investigation of anisotropic superconducting spin transport at a magnetic interface between a p -wave superconductor and a ferromagnetic insulator. Our formulation describes the ferromagnetic resonance modulations due to spin current generation depending on spin-triplet Cooper pair, including the frequency shift and enhanced Gilbert damping, in a unified manner. We find that the Cooper pair symmetry is detectable from the qualitative behavior of the ferromagnetic resonance modulation. Our theory paves the way toward anisotropic superconducting spintronics.

DOI: [10.1103/PhysRevB.106.L161406](https://doi.org/10.1103/PhysRevB.106.L161406)

Introduction. Use of spin-triplet Cooper pairs as carriers for spin currents in the emergent field of superconducting spintronics is challenging [1,2]. Previous studies have demonstrated spin transport mediated by spin-triplet Cooper pairs that formed at the s -wave superconductor (SC)/ferromagnet interfaces of Josephson junctions. The spin-singlet pairs in SCs are converted into spin-triplet pairs in half-metallic CrO₂ [3]. However, previous studies on spin-triplet pairs at magnetic interfaces have been limited to cases induced by the proximity effect.

One promising candidate material system for investigation of spin-triplet currents to enable more active use of spin-triplet pairs is the p -wave SC/ferromagnetic insulator (FI) bilayer thin film system [4,5]. Tunneling of the spins is driven by the magnetization dynamics excited by ferromagnetic resonance (FMR) in the ferromagnetic material via interfacial exchange coupling between the magnetization in the FI and the electron spins in the p -wave SC, and a spin-triplet current is expected to be generated. Furthermore, as a backaction of spin injection, both the FMR frequency and the Gilbert damping of the FI should be modulated [6–8]. Although similar scenarios have already been studied vigorously in s -wave SC/ferromagnet systems, most previous studies have focused on the Gilbert damping modulation due to spin injection [9–22]. To gain an in-depth understanding of the spin-triplet transport mechanisms, the FMR modulation processes, including both the frequency shift and the enhanced Gilbert damping, should be formulated microscopically in a systematic manner.

Determination of the pairing symmetry of the spin-triplet p -wave SCs within the same framework is also desirable. Despite many years of research based on several experimental techniques that detect the pairing symmetry, including nuclear magnetic resonance [23], polarized neutron scattering [24–26], and muon-spin resonance techniques [27], there

are few established candidate systems for spin-triplet SCs [28–32]. The FMR modulation has been observed in various nanoscale magnetic multilayers. Accordingly, the technique is widely used to investigate a spin transport property in a variety of nanoscale thin film systems because it is highly sensitive. Thus one can expect that the FMR measurements in p -wave SC/FI bilayer systems provide useful information about pairing symmetry.

In this Letter, we investigate anisotropic superconducting spin transport at the magnetic interfaces of hybrid systems composed of p -wave SC/FI thin films theoretically, as illustrated in Fig. 1(a). The two-dimensional bulk SC is placed on the FI, where the FMR occurs. The precession axis is rotated by an angle θ from the direction perpendicular to the interface. Here, we use two coordinate systems: (x, y, z) and (X, Y, Z) . The z axis is perpendicular to the interface and the x and y axes are along the interface. The (X, Y, Z) coordinate is obtained by rotating the angle θ around the y axis, so that the precession axis and the Z axis are parallel. Figure 1(b) shows a schematic image of the spin-triplet Cooper pairs for the chiral and helical p -wave SCs considered in this work. Figure 1(c) shows a schematic image of the FMR signal in the FI monolayer and the SC/FI bilayer. The FMR frequency and linewidth in the SC/FI bilayer are both modulated because of the spin transfer occurring at the interface.

Using the nonequilibrium Green's function method, we formulate the FMR modulations due to the backaction of the spin-triplet transport process systematically. The main advantage of using the nonequilibrium Green's function is dealing with both a spectral function and a nonequilibrium distribution function. Indeed, the interface spin current is given by the expression using the nonequilibrium distribution function, which shows that the interface spin current by the spin pumping and the enhanced Gilbert damping are proportional to each other. Furthermore, as an advantage of field theoretical

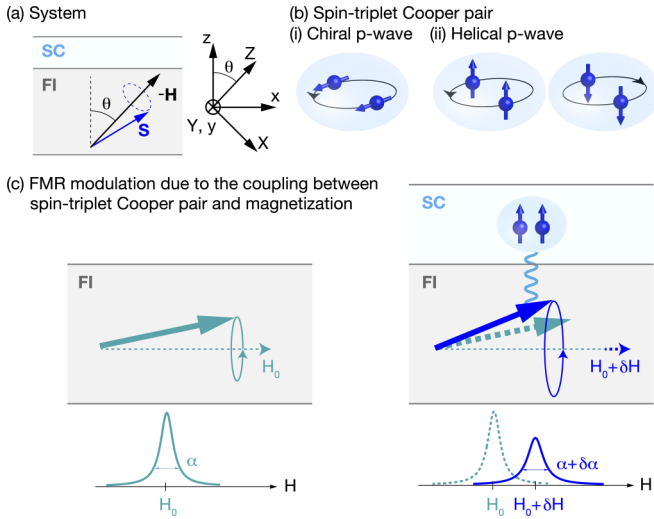


FIG. 1. Mechanism of FMR modulation due to anisotropic superconducting spin transport at magnetic interfaces. (a) Precession axis located on the x - z plane, where the angle between the precession axis and the z axis is θ (where $0 \leq \theta \leq \pi/2$). (b) Two types of spin-triplet Cooper pairs considered in this work. (c) FMR signal modulation in the SC/FI bilayer system compared with the signal in the FI monolayer.

treatment, the frequency shift and the enhanced Gilbert damping are both described in a unified manner. Additionally, it is shown that the symmetry of the spin-triplet pairs can be extracted from the FMR modulations. The results presented here offer a pathway toward development of anisotropic superconducting spintronics.

Model Hamiltonian. The FMR modulation due to the SC adjacent to the FI is calculated microscopically using the spin tunneling Hamiltonian method [9–11,33–38]. The effect of the SC on the FI is treated as a perturbation and suppression of ferromagnetism with the onset of superconductivity is assumed to be negligible, which is consistent with the results of spin pumping experiments in magnetic multilayer thin films. The details of the model Hamiltonians and the formulations are described in the Supplemental Material [39]. In the main text, we focus on giving an overview of the model Hamiltonians and the formulations.

The total Hamiltonian $H(t)$ comprises three terms

$$H(t) = H_{\text{FI}}(t) + H_{\text{SC}} + H_{\text{ex}}. \quad (1)$$

The first term $H_{\text{FI}}(t)$ describes the bulk FI,

$$H_{\text{FI}}(t) = \sum_{\mathbf{k}} \hbar\omega_{\mathbf{k}} b_{\mathbf{k}}^{\dagger} b_{\mathbf{k}} - h_{\text{ac}}^{+}(t) b_{\mathbf{k}=0}^{\dagger} - h_{\text{ac}}^{-}(t) b_{\mathbf{k}=0}, \quad (2)$$

where $b_{\mathbf{k}}^{\dagger}$ and $b_{\mathbf{k}}$ denote the creation and annihilation operators of magnons with the wave vector $\mathbf{k} = (k_x, k_y, k_z)$, respectively. We assume the parabolic dispersion $\hbar\omega_{\mathbf{k}} = Dk^2 - \hbar\gamma H$, where $\gamma (< 0)$ is the electron gyromagnetic ratio. The coupling between the microwave radiation and the magnons is given by $h_{\text{ac}}^{\pm}(t) = \hbar\gamma h_{\text{ac}} \sqrt{SN/2} e^{\mp i\omega t}$, where h_{ac} and ω are the amplitude and the frequency of the microwave radiation, respectively. S is the magnitude of the localized spin and N is the number of sites in the FI. Note that the precession axis for the localized spin is fixed along the Z axis [see Fig. 1(a)].

The second term H_{SC} describes the two-dimensional bulk SCs,

$$H_{\text{SC}} = \frac{1}{2} \sum_{\mathbf{k}} c_{\mathbf{k}}^{\dagger} H_{\text{BdG}} c_{\mathbf{k}}, \quad (3)$$

where we use the four-component notations

$$c_{\mathbf{k}}^{\dagger} = (c_{k\uparrow}^{\dagger}, c_{k\downarrow}^{\dagger}, c_{-k\uparrow}, c_{-k\downarrow}), \quad (4)$$

$$c_{\mathbf{k}} = (c_{k\uparrow}, c_{k\downarrow}, c_{-k\uparrow}^{\dagger}, c_{-k\downarrow}^{\dagger})^T. \quad (5)$$

Here, $c_{k_s}^{\dagger}$ and c_{k_s} denote creation and annihilation operators, respectively, of electrons with the wave vector $\mathbf{k} = (k_x, k_y)$ and the z component of the spin $s = \uparrow, \downarrow$. The Bogoliubov–de Gennes Hamiltonian H_{BdG} is a 4×4 matrix given by

$$H_{\text{BdG}} = \begin{pmatrix} \xi_{\mathbf{k}} \sigma^0 & \Delta_{\mathbf{k}} \\ -\Delta_{\mathbf{k}}^* & -\xi_{\mathbf{k}} \sigma^0 \end{pmatrix}, \quad (6)$$

where $\xi_{\mathbf{k}}$ represents the energy of the electrons as measured from their chemical potential, σ^0 is a 2×2 unit matrix, and the pairing potential $\Delta_{\mathbf{k}}$ is also a 2×2 matrix. We consider three pairing potential types, including the spin-singlet s -wave pairing $\Delta_{\mathbf{k}} = \Delta i\sigma^y$ and two spin-triplet p -wave pairings $\Delta_{\mathbf{k}} = (\mathbf{d}_{\mathbf{k}} \cdot \boldsymbol{\sigma}) i\sigma^y$, where their \mathbf{d} vectors are given by

$$\mathbf{d}_{\mathbf{k}} = \begin{cases} \Delta(0, 0, e^{i\phi_{\mathbf{k}}}) : & \text{chiral } p \text{ wave,} \\ \Delta(-\sin \phi_{\mathbf{k}}, \cos \phi_{\mathbf{k}}, 0) : & \text{helical } p \text{ wave,} \end{cases} \quad (7)$$

where $\phi_{\mathbf{k}} = \arctan(k_y/k_x)$ is an azimuth angle. The phenomenological form of the gap function is assumed,

$$\Delta = 1.76 k_B T_c \tanh(1.74 \sqrt{T_c/T - 1}), \quad (8)$$

with T_c the superconducting transition temperature. By diagonalizing H_{BdG} , the quasiparticle energy is given by $E_{\mathbf{k}} = \sqrt{\xi_{\mathbf{k}}^2 + \Delta^2}$ for all SCs considered here. Therefore, one cannot distinguish them by the energy spectrum alone, and they are simple models suitable for studying the difference of the magnetic responses due to the pairing symmetry [40].

The third term H_{ex} represents the proximity exchange coupling that occurs at the interface, which describes the spin transfer between the SC and the FI [10,33],

$$H_{\text{ex}} = \sum_{q,\mathbf{k}} (J_{q,\mathbf{k}} \sigma_q^+ S_{\mathbf{k}}^- + \text{H.c.}), \quad (9)$$

where $J_{q,\mathbf{k}}$ is the matrix element for the spin transfer processes, $\sigma_q^{\pm} = (\sigma_q^x \pm i\sigma_q^y)/2$ represent the spin-flip operators for the electron spins in the SCs, and $S_{\mathbf{k}}^- = \sqrt{2S} b_{\mathbf{k}}^{\dagger}$ and $S_{\mathbf{k}}^+ = \sqrt{2S} b_{\mathbf{k}}$ represent the Fourier component of the localized spin in the FI. Note that the precession axis is along the Z axis, so that the Z component of the spin is injected into the SC when the FMR occurs. Using the creation and annihilation operators of electrons and magnons, H_{ex} is written as

$$H_{\text{ex}} = \sum_{q,\mathbf{k},\mathbf{k}',s,s'} (\sqrt{2S} J_{q,\mathbf{k}} \sigma_{ss'}^+ c_{\mathbf{k}'s}^{\dagger} c_{\mathbf{k}+q,s'} b_{-\mathbf{k}}^{\dagger} + \text{H.c.}). \quad (10)$$

From the above expression, one can see that H_{ex} describes electron scattering processes with magnon emission and absorption.

Modulation of FMR. The FMR modulation can be read from the retarded component of the magnon Green's function [33], which is given by

$$G_k^R(\omega) = \frac{2S/\hbar}{\omega - \omega_k + i\alpha\omega - (2S/\hbar)\Sigma_k^R(\omega)}, \quad (11)$$

where the Gilbert damping constant α is introduced phenomenologically [41–43]. In the second-order perturbation calculation with respect to the matrix element $J_{q,k}$, the self-energy caused by proximity exchange coupling is given by

$$\Sigma_k^R(\omega) = - \sum_q |J_{q,k}|^2 \chi_q^R(\omega), \quad (12)$$

where the dynamic spin susceptibility of the SCs is defined as

$$\chi_q^R(\omega) := \int dt e^{i(\omega+i0)t} \frac{i}{\hbar} \theta(t) \langle [\sigma_q^+(t), \sigma_{-q}^-(0)] \rangle. \quad (13)$$

The pole of $G_k^R(\omega)$ indicates the FMR modulation, i.e., the shift of resonance frequency and the enhancement of the Gilbert damping. By solving the equation

$$\omega - \omega_{k=0} - (2S/\hbar)\text{Re}\Sigma_{k=0}^R(\omega) = 0, \quad (14)$$

at a fixed microwave frequency ω , one obtains the magnetic field at which the FMR occurs. The imaginary part of the self-energy gives the enhancement of the Gilbert damping. Consequently, the frequency shift and the enhanced Gilbert damping are given by

$$\delta H = \frac{2S}{\gamma\hbar} \text{Re}\Sigma_{k=0}^R(\omega), \quad \delta\alpha = -\frac{2S}{\hbar\omega} \text{Im}\Sigma_{k=0}^R(\omega). \quad (15)$$

From the above equations and Eq. (12), one can see that the FMR modulation provides information about both the interface coupling properties and the dynamic spin susceptibility of the SCs.

The form of matrix element $J_{q,k=0}$ depends on the details of the interface. In this work, we assume the interface with uncorrelated roughness. $|J_{q,k=0}|^2$ is given by

$$|J_{q,k=0}|^2 = \frac{J_1^2}{N} \delta_{q,0} + \frac{J_2^2 l^2}{NA}, \quad (16)$$

where the first and second terms describe averaged uniform contribution and uncorrelated roughness contribution, respectively [39]. J_1 and J_2 correspond to the mean value and variance, respectively. A is the area of the interface, which is equal to the system size of the SC. l is an atomic scale length. Using Eq. (16), the self-energy for the uniform magnon mode is given by

$$\Sigma_{k=0}^R(\omega) = -\frac{J_1^2}{N} \chi_{\text{uni}}^R(\omega) - \frac{J_2^2 l^2}{NA} \chi_{\text{loc}}^R(\omega), \quad (17)$$

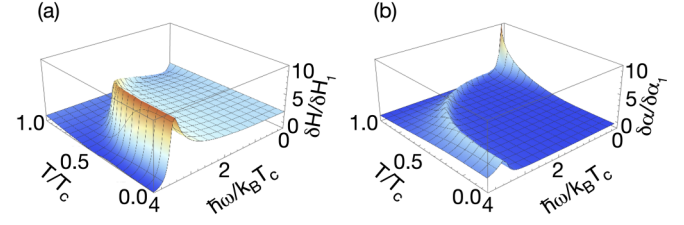
where the uniform and local spin susceptibilities are defined as

$$\chi_{\text{uni}}^R(\omega) := \lim_{|q| \rightarrow 0} \chi_q^R(\omega), \quad \chi_{\text{loc}}^R(\omega) := \sum_q \chi_q^R(\omega). \quad (18)$$

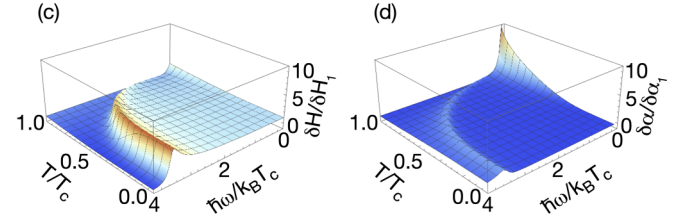
The self-energy $\Sigma_{k=0}^R(\omega)$ consists of two terms originating from the uniform and roughness contributions, so that both $\chi_{\text{uni}}^R(\omega)$ and $\chi_{\text{loc}}^R(\omega)$ contribute to δH and $\delta\alpha$.

Here, we discuss the FI thickness dependence on the FMR modulation [44]. From Eqs. (15), and (17), one can see that

Chiral p -wave $\Gamma/k_B T_c = 0.05$



Helical p -wave $\Gamma/k_B T_c = 0.05$



s -wave $\Gamma/k_B T_c = 0.05$

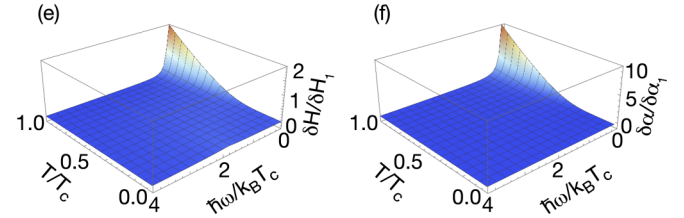


FIG. 2. Frequency shift δH and the enhanced Gilbert damping $\delta\alpha$ as a function of temperature and frequency normalized by the characteristic values $\delta H_1 = -SJ_1^2 D_F / (N\gamma\hbar)$ and $\delta\alpha_1 = SJ_1^2 D_F / (Nk_B T_c)$ in the normal state. D_F ($\propto A$) is the density of states at the Fermi level in the normal state. We set $\theta = 0$ and $\Gamma/k_B T_c = 0.05$. The sign of δH corresponds to the sign of $\text{Re}\chi_{\text{uni}}^R(\omega)$, which can be positive and negative at low and high frequencies, respectively. In contrast, $\delta\alpha$ is positive at any frequency.

the FMR modulation is inversely proportional to the FI thickness ($\propto A/N$) because $\chi_{\text{uni}}^R(\omega) \propto A$ and $\chi_{\text{loc}}^R(\omega) \propto A^2$. This is consistent with the experiments on the spin pumping in $\text{Y}_3\text{Fe}_5\text{O}_{12}/\text{Pt}$ heterostructures [45]. In order to observe the FMR modulation experimentally, it is necessary to prepare a sample that is sufficiently thin, e.g., typically, the thickness of several tens of nanometers.

Numerical results. In the following, we consider a flat interface where $J_2 = 0$, so that the behavior of the FMR modulation is determined by $\chi_{\text{uni}}^R(\omega)$. The roughness contribution proportional to $\chi_{\text{loc}}^R(\omega)$ is discussed later. Figure 2 shows the frequency shift δH and the enhanced Gilbert damping $\delta\alpha$ as a function of temperature and frequency. Here, we set $\theta = 0$ and $\Gamma/k_B T_c = 0.05$, where Γ is a constant level broadening of the quasiparticle introduced phenomenologically [39].

First, we explain the qualitative properties of δH and $\delta\alpha$ for the chiral p -wave SC. In the low frequency region, where $\hbar\omega/k_B T_c \leq 1$, δH is finite and remains almost independent of ω near the zero temperature and $\delta\alpha$ decreases and becomes exponentially small with the decrease of the temperature. In the high frequency region, where $\hbar\omega/k_B T_c \geq 1$, a resonance peak occurs at $\hbar\omega = 2\Delta$ for both δH and $\delta\alpha$. The qualitative properties of δH and $\delta\alpha$ for the helical p -wave SC are the same as those of the chiral p -wave SC.

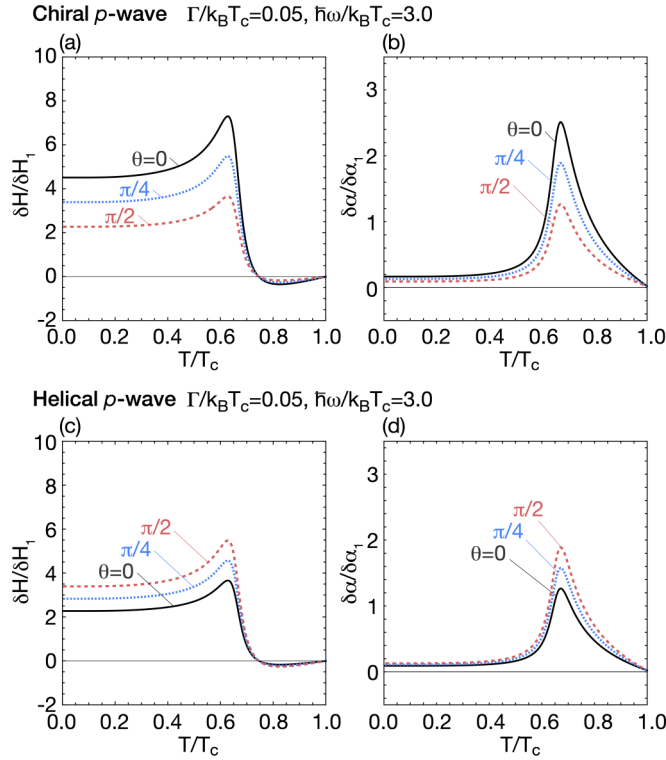


FIG. 3. Frequency shift and the enhanced Gilbert damping as a function of temperature at angles of $\theta = 0, \pi/4, \pi/2$. The upper and lower panels show the characteristics for the chiral and helical p -wave SCs, respectively.

Next, we explain the qualitative properties of δH and $\delta\alpha$ for the s -wave SC. In the low frequency region, where $\hbar\omega/k_B T_c \leq 1$, both δH and $\delta\alpha$ decrease and become exponentially small with the decrease of the temperature. In the high frequency region, where $\hbar\omega/k_B T_c \geq 1$, both δH and $\delta\alpha$ vanish.

The p -wave SCs show two characteristic properties that the s -wave SC does not show: a finite δH at $T = 0$ and a resonance peak of δH and $\delta\alpha$. These properties can be understood by the analogy between SCs and band insulators as follows. The uniform dynamic spin susceptibility consists of contributions from intraband transitions within particle (hole) bands and interband transitions between particles and holes. In the low temperature or high frequency region, the intraband contribution is negligible and the interband contribution is dominant. In the case of the s -wave SC, the interband transitions are forbidden because the Hamiltonian and the spin operator commute. As a result, there is no spin response in the low-temperature or high-frequency regions. In contrast, the Hamiltonian for the p -wave SCs and the spin operator do not commute. Therefore, δH has a finite value near-zero temperature due to the interband contribution. In addition, a resonance peak occurs when $\hbar\omega = 2\Delta$ because the density of states diverges at the band edge $E = \pm\Delta$. A detailed proof of the above statement is given in the Supplemental Material [39].

The angle dependences of δH and $\delta\alpha$ are distinct for chiral and helical p -wave SCs, as shown in Fig. 3. In both cases, we set $\hbar\omega/k_B T_c = 3.0$ as the typical values at high frequencies, where the main contribution of the uniform spin susceptibility

TABLE I. FMR modulation properties for the flat SC/FI interface where $J_1 \neq 0$ and $J_2 = 0$.

| Pairing symmetry | s | Chiral | Helical |
|--|-----|----------|----------|
| δH in the limit of $T \rightarrow 0$ | 0 | Finite | Finite |
| Resonance peak of $\delta H, \delta\alpha$ | | ✓ | ✓ |
| $\partial_\theta(\delta H), \partial_\theta(\delta\alpha)$ | 0 | Negative | Positive |

is the interband transitions. In the chiral p -wave SC, δH and $\delta\alpha$ tend to decrease and are halved at a fixed temperature when θ increases from 0 to $\pi/2$. Conversely, in the helical p -wave SC, the qualitative behavior shows the opposite trend. δH and $\delta\alpha$ both tend to increase and become 1.5 times larger at a fixed temperature when θ increases from 0 to $\pi/2$. In fact, the angle dependences are approximately obtained to be $\propto 1 + \cos^2 \theta$ and $1 + (\sin^2 \theta)/2$ for chiral and helical p -wave SCs, respectively [39]. Therefore, the spin configuration of the Cooper pair can be detected from the θ dependence data for the FMR modulation.

The FMR modulation properties of the three SCs are summarized in Table I. All SCs considered here can be distinguished based on three properties: the frequency shift in the low temperature limit, the presence of their resonance peak, and their θ dependence. For the s -wave SC, δH becomes exponentially small in $T \rightarrow 0$, while for the p -wave SCs, δH is finite in $T \rightarrow 0$. For the s -wave SC, δH and $\delta\alpha$ show no resonance and no θ dependence, while for the chiral and helical p -wave SCs, both δH and $\delta\alpha$ exhibit a resonance at $\hbar\omega = 2\Delta$ and a θ dependence. In addition, these two p -wave SCs can be distinguished from their θ dependences of δH and $\delta\alpha$, which are characterized by $\partial_\theta(\delta H)$ and $\partial_\theta(\delta\alpha)$, respectively. Here, it should be emphasized that the pairing symmetry can be characterized by the sign of $\partial_\theta(\delta H)$ and $\partial_\theta(\delta\alpha)$. These properties are summarized in the Table I.

Spin-triplet current generation. The relationship between the enhanced Gilbert damping discussed above and the spin-triplet current generation must also be discussed. The enhancement of the Gilbert damping is known to originate from the spin current generation at the magnetic interface [6,33]. The interface spin current induced by FMR $\langle I_S \rangle^{\text{SP}}$ is given by [39]

$$\langle I_S \rangle^{\text{SP}} = \frac{N(\hbar\gamma h_{\text{ac}})^2}{2\alpha} [-\text{Im}G_{\mathbf{k}=\mathbf{0}}^R(\omega)]\delta\alpha. \quad (19)$$

One can see that $\langle I_S \rangle^{\text{SP}}$ and $\delta\alpha$ are proportional to each other. In our setup, the enhanced Gilbert damping $\delta\alpha$ will lead to the generation of both the Cooper pair spin-triplet current and the quasiparticle spin current. Since the angular dependence of $\delta\alpha$ reflects the direction of the Cooper pair spins, it is expected that the spin-triplet current can be controlled by varying the magnetization direction of the FI.

Discussion. We have considered a flat SC/FI interface. In the presence of roughness, the correction term proportional to $\chi_{\text{loc}}^R(\omega)$ contributes to the FMR modulation, as shown in Eq. (17). In the rough limit, $J_1^2 \ll J_2^2$, $\chi_{\text{loc}}^R(\omega)$ dominates to make the FMR modulation isotropic, due to the angle average by summation over \mathbf{q} . Namely, the anisotropy peculiar to p -wave SC is smeared by the roughness. The detailed behavior

of $\chi_{\text{loc}}^R(\omega)$ is shown in the Supplemental Material [39]. This result implies that it is crucial to control the interface roughness. In principle, the roughness of the interface can be observed using transmission electron microscopy of interfaces [46–48] and it is possible to detect whether the interface of the sample is flat or rough. More detailed spectroscopy can be obtained from the FMR modulation by using a flat interface.

Our results show that the pairing symmetry can be detected by the sign of $\partial_\theta(\delta H)$ and $\partial_\theta(\delta\alpha)$ around the in-plane magnetic field ($\theta \sim \pi/2$), where the vortices are negligible. When the external magnetic field has a large out-of-plane component, the vortex formation may cause problems in observing the angular dependence. The qualitative behavior is expected to change when the out-of-plane magnetic field approaches the upper critical field ($H \sim H_{c2} \sim 1$ T). This is because the coherence length of the Cooper pair and the distance between the vortices can become comparable. Indeed, it has been experimentally reported that the vortex formation suppresses the characteristic properties in the spin pumping into SCs [20]. Therefore, the out-of-plane magnetic field should be as small as possible when FMR measurements are performed for $H \sim H_{c2}$.

Recent experiments have reported that UTe_2 is a candidate material for spin-triplet p -wave SCs [31], which has attracted a great deal of attention. Various experiments, including spectroscopic measurements, are now in progress to investigate the pairing symmetry of UTe_2 and indicated that the superconducting transition temperature is about $1 \text{ K} \sim 30 \text{ GHz}$. Therefore, the resonance condition $\hbar\omega = 2\Delta$ shown above is accessible to recent broadband FMR measurements.

In addition, experiments on spin pumping into d -wave SCs have recently been reported [49] and a theoretical investigation of the enhancement of the Gilbert damping in a d -wave SC/FI bilayer system

has recently been presented [50]. Thus anisotropic superconducting spintronics can be expected to develop as a new research direction.

We should emphasize two important aspects of the FMR method presented here: the spectroscopic probe method for the p -wave SC thin films and the versatile spin injection method. First, the FMR measurement procedure can provide a new spin-sensitive measurement method that will complement other measurement methods to enable a breakthrough in the discovery of spin-triplet SCs. Second, the FMR method represents a promising way to generate spin-triplet currents in p -wave SC thin films.

Conclusions. We have investigated the anisotropic superconducting spin transport at magnetic interfaces composed of a p -wave SC and an FI based on a microscopic model Hamiltonian. The FMR signal in these p -wave SC/FI bilayer systems is modulated via spin transfer at the interface, which generates spin-triplet currents. We have shown that the pairing symmetry of the SCs can be extracted from the FMR modulation characteristics. Our approach provides a unique way to explore anisotropic superconducting spintronics, which will be useful for application to emerging device technologies.

Note added. Recently, we became aware of a closely related work, where a way to convert spin-triplet currents to magnon spin currents in SC/FI bilayer systems is discussed [51].

We thank R. Ohshima, M. Shiraishi, H. Chudo, G. Okano, K. Yamanoi, and Y. Nozaki for helpful discussions. This work was supported by the Priority Program of the Chinese Academy of Sciences under Grant No. XDB28000000, and by JSPS KAKENHI under Grants No. JP20K03835, No. JP20H04635, No. JP20H01863, No. JP21H04565, and No. JP21H01800.

-
- [1] J. Linder and J. W. A. Robinson, *Nat. Phys.* **11**, 307 (2015).
 [2] W. Han, S. Maekawa, and X.-C. Xie, *Nat. Mater.* **19**, 139 (2020).
 [3] R. S. Keizer, S. T. B. Goennenwein, T. M. Klapwijk, G. Miao, G. Xiao, and A. Gupta, *Nature (London)* **439**, 825 (2006).
 [4] Y. Tanaka, T. Yokoyama, A. V. Balatsky, and N. Nagaosa, *Phys. Rev. B* **79**, 060505(R) (2009).
 [5] P. M. R. Brydon, *Phys. Rev. B* **80**, 224520 (2009).
 [6] Y. Tserkovnyak, A. Brataas, and G. E. W. Bauer, *Phys. Rev. Lett.* **88**, 117601 (2002).
 [7] Y. Tserkovnyak, A. Brataas, G. E. W. Bauer, and B. I. Halperin, *Rev. Mod. Phys.* **77**, 1375 (2005).
 [8] E. Šimánek and B. Heinrich, *Phys. Rev. B* **67**, 144418 (2003).
 [9] M. Inoue, M. Ichioka, and H. Adachi, *Phys. Rev. B* **96**, 024414 (2017).
 [10] T. Kato, Y. Ohnuma, M. Matsuo, J. Rech, T. Jonckheere, and T. Martin, *Phys. Rev. B* **99**, 144411 (2019).
 [11] M. A. Silaev, *Phys. Rev. B* **102**, 144521 (2020).
 [12] M. A. Silaev, *Phys. Rev. B* **102**, 180502(R) (2020).
 [13] R. Ojajarvi, J. Manninen, T. T. Heikkilä, and P. Virtanen, *Phys. Rev. B* **101**, 115406 (2020).
 [14] H. T. Simensen, L. G. Johnsen, J. Linder, and A. Brataas, *Phys. Rev. B* **103**, 024524 (2021).
 [15] C. Bell, S. Milikisyants, M. Huber, and J. Aarts, *Phys. Rev. Lett.* **100**, 047002 (2008).
 [16] K.-R. Jeon, C. Ciccarelli, A. J. Ferguson, H. Kurebayashi, L. F. Cohen, X. Montiel, M. Eschrig, J. W. A. Robinson, and M. G. Blamire, *Nat. Mater.* **17**, 499 (2018).
 [17] Y. Yao, Q. Song, Y. Takamura, J. P. Cascales, W. Yuan, Y. Ma, Y. Yun, X. C. Xie, J. S. Moodera, and W. Han, *Phys. Rev. B* **97**, 224414 (2018).
 [18] L.-L. Li, Y.-L. Zhao, X.-X. Zhang, and Y. Sun, *Chin. Phys. Lett.* **35**, 077401 (2018).
 [19] K.-R. Jeon, C. Ciccarelli, H. Kurebayashi, L. F. Cohen, X. Montiel, M. Eschrig, T. Wagner, S. Komori, A. Srivastava, J. W. A. Robinson, and M. G. Blamire, *Phys. Rev. Appl.* **11**, 014061 (2019).
 [20] K.-R. Jeon, C. Ciccarelli, H. Kurebayashi, L. F. Cohen, S. Komori, J. W. A. Robinson, and M. G. Blamire, *Phys. Rev. B* **99**, 144503 (2019).
 [21] I. Golovchanskiy, N. Abramov, V. Stolyarov, V. Chichkov, M. Silaev, I. Shchetinin, A. Golubov, V. Ryazanov, A. Ustinov, and M. Kupriyanov, *Phys. Rev. Appl.* **14**, 024086 (2020).

- [22] Y. Zhao, Y. Yuan, K. Fan, and Y. Zhou, *Appl. Phys. Express* **13**, 033002 (2020).
- [23] A. J. Leggett, *Rev. Mod. Phys.* **47**, 331 (1975).
- [24] C. G. Shull and R. P. Ferrier, *Phys. Rev. Lett.* **10**, 295 (1963).
- [25] C. G. Shull, *Phys. Rev. Lett.* **10**, 297 (1963).
- [26] C. G. Shull and F. A. Wedgwood, *Phys. Rev. Lett.* **16**, 513 (1966).
- [27] G. M. Luke, A. Keren, L. P. Le, W. D. Wu, Y. J. Uemura, D. A. Bonn, L. Taillefer, and J. D. Garrett, *Phys. Rev. Lett.* **71**, 1466 (1993).
- [28] S. S. Saxena, P. Agarwal, K. Ahilan, F. M. Grosche, R. K. W. Haselwimmer, M. J. Steiner, E. Pugh, I. R. Walker, S. R. Julian, P. Monthoux, G. G. Lonzarich, A. Huxley, I. Sheikin, D. Braithwaite, and J. Flouquet, *Nature (London)* **406**, 587 (2000).
- [29] D. Aoki, A. Huxley, E. Ressouche, D. Braithwaite, J. Flouquet, J.-P. Brison, E. Lhotel, and C. Paulsen, *Nature (London)* **413**, 613 (2001).
- [30] N. T. Huy, A. Gasparini, D. E. de Nijs, Y. Huang, J. C. P. Klaasse, T. Gortenmulder, A. de Visser, A. Hamann, T. Görlach, and H. v. Löhneysen, *Phys. Rev. Lett.* **99**, 067006 (2007).
- [31] S. Ran, C. Eckberg, Q.-P. Ding, Y. Furukawa, T. Metz, S. R. Saha, I.-L. Liu, M. Zic, H. Kim, J. Paglione, and N. P. Butch, *Science* **365**, 684 (2019).
- [32] J. Yang, J. Luo, C. Yi, Y. Shi, Y. Zhou, and G.-q. Zheng, *Sci. Adv.* **7**, eabl4432 (2021).
- [33] Y. Ohnuma, H. Adachi, E. Saitoh, and S. Maekawa, *Phys. Rev. B* **89**, 174417 (2014).
- [34] Y. Ohnuma, M. Matsuo, and S. Maekawa, *Phys. Rev. B* **96**, 134412 (2017).
- [35] G. Tatara and S. Mizukami, *Phys. Rev. B* **96**, 064423 (2017).
- [36] M. Matsuo, Y. Ohnuma, T. Kato, and S. Maekawa, *Phys. Rev. Lett.* **120**, 037201 (2018).
- [37] Y. Ominato and M. Matsuo, *J. Phys. Soc. Jpn.* **89**, 053704 (2020).
- [38] Y. Ominato, J. Fujimoto, and M. Matsuo, *Phys. Rev. Lett.* **124**, 166803 (2020).
- [39] See Supplemental Material at <http://link.aps.org/supplemental/10.1103/PhysRevB.106.L161406> for details of the model derivation, formulation, and calculations.
- [40] M. Sigrist and K. Ueda, *Rev. Mod. Phys.* **63**, 239 (1991).
- [41] T. Kasuya and R. C. LeCraw, *Phys. Rev. Lett.* **6**, 223 (1961).
- [42] V. Cherepanov, I. Kolokolov, and V. L'vov, *Phys. Rep.* **229**, 81 (1993).
- [43] L. Jin, Y. Wang, G. Lu, J. Li, Y. He, Z. Zhong, and H. Zhang, *AIP Adv.* **9**, 025301 (2019).
- [44] W. Chen, M. Sigrist, J. Sinova, and D. Manske, *Phys. Rev. Lett.* **115**, 217203 (2015).
- [45] M. B. Jungfleisch, A. V. Chumak, A. Kehlberger, V. Lauer, D. H. Kim, M. C. Onbasli, C. A. Ross, M. Kläui, and B. Hillebrands, *Phys. Rev. B* **91**, 134407 (2015).
- [46] Z. Qiu, K. Ando, K. Uchida, Y. Kajiwara, R. Takahashi, H. Nakayama, T. An, Y. Fujikawa, and E. Saitoh, *Appl. Phys. Lett.* **103**, 092404 (2013).
- [47] L. Mihalceanu, S. Keller, J. Greser, D. Karfaridis, K. Simeonidis, G. Vourlias, T. Kehagias, A. Conca, B. Hillebrands, and E. T. Papaioannou, *Appl. Phys. Lett.* **110**, 252406 (2017).
- [48] Ikhtiar, H. Sukegawa, X. Xu, M. Belmoubarik, H. Lee, S. Kasai, and K. Hono, *Appl. Phys. Lett.* **112**, 022408 (2018).
- [49] S. J. Carreira, D. Sanchez-Manzano, M.-W. Yoo, K. Seurre, V. Rouco, A. Sander, J. Santamaría, A. Anane, and J. E. Villegas, *Phys. Rev. B* **104**, 144428 (2021).
- [50] Y. Ominato, A. Yamakage, T. Kato, and M. Matsuo, *Phys. Rev. B* **105**, 205406 (2022).
- [51] L. G. Johnsen, H. T. Simensen, A. Brataas, and J. Linder, *Phys. Rev. Lett.* **127**, 207001 (2021).